IMPROVED SHALLOW CUMULUS PROCESS IN THE CENTRAL WEATHER BUREAU GLOBAL FORECAST SYSTEM

[1]Jui-Lin F. Li and [2]Feng-Ju Wang

[1]Department of Atmospheric Science, UCLA, USA
[2]RDC, Central Weather Bureau

ABSTRACT

Shallow non-precipitating cumulus scheme used in the Global Forecast System (GFS) of the Central Weather Bureau (CWB) is revised and tested both with a single column and a full-coupled version of the model.

It has been reported that the low-level horizontal water vapor transports were not sufficient and the geographical patterns of precipitation rates were not well simulated by the GFS. The simulated summer precipitation rates exhibited excessive values over subtropical western Pacific and underestimated rates over eastern equatorial Pacific. These could be due to the shallow cumulus processes are not well formulated in the model. Results from tests with a single column version of the GFS indicate that the scheme fails to maintain observed shallow cumulus cloud planetary boundary layers (PBLs) forced by shallow cloud regimes of BOMEX. The scheme only considers local cumulus diffusion and ignores important condensation-evaporation cycle, which is crucial to maintain a shallow cumulus cloud by resupplying water vapor in the cloud layer.

In this paper, we present an alternative, which is a simple eddy diffusive scheme with a nonlocal transfers inclusion. This scheme, following Li and Young (1993), is diagnostic and consists of two components: it represents the cumulus fluxes of liquid water potential temperature and total water as the sum of local diffusion plus nonlocal convection. It estimates the cumulus diffusivities from cloud available potential energy with an empirical nonlocal flux component derived from a large eddy simulation (LES) data. The shallow cumulus cloud layer is well maintained initialized by BOMEX condition with the new scheme in the single column tests. Preliminary results simulated using the new scheme but with a full-coupled version are very encouraging; the geographical distributions of July precipitation rates, sea level pressure and surface latent heat flux etc show more realistic pattern and values than that of the current scheme of the GFS. We will present some of the results in the meeting.

(Key words: Planetary boundary layer, shallow cumulus clouds, local and nonlocal turbulent transfers)

1. INTRODUCTION

Shallow non-precipitating cumulus clouds play an important role in the global hydrological cycle (Riehl et al. 1951). The shallow clouds form in the upper portion of the planetary boundary layer (PBL) and play an important role in enhancing mixing and deepening of it. These situations can be found over the humid daytime fair-weather boundary layer in land, the trade wind PBL in subtropical oceans and the cold airmass flowing over a warmer sea (CAO) in midlatitudes. Usually, the accumulated heat and water vapor destabilize the PBL and enhance the possibility of cumulus convection within it. Initially the water vapor is transported upward, released as latent heat in shallow cumulus clouds, and reevaporated near their top. This condensation-evaporation cycle helps to maintain a conditionally unstable cloud layer with an internal maximum of buoyancy flux. Without considering shallow convection models often have PBLs that are too shallow with too weak surface turbulent fluxes and is inconsistent with the timely development of subsequent deep cumulus convection.

Active shallow cumulus clouds can be thought of as large thermals from the surface layer which are able to penetrate well above their level of free convection (LFC); hence they are the roots for cumulus convection (LeMone and Pennel 1976). These cumulus motions, in general, are expected to have strong updraft, which therefore may not be locally downgradient in vertical. These cumulus nonlocal transports are strongly coupled to subcloud layer.

Recently, simple shallow cumulus parameterizations have been developed and used in general circulation models (GCMs). They include simple eddy diffusion scheme (Tiedtke 1984), Betts-Miller adjustment scheme (Betts and Miller 1986), and the mass flux scheme (Tiedtke 1989). Each of them has deficiencies when applied to strongly convective situations. For example, cloud root effects on the subcloud layer have been inadequately represented. The simple diffusion scheme only considers local transfers. The Betts-Miller scheme is usually downgradient. The mass flux scheme has been closed by a moisture flux assumption that ignores sensible heat fluxes. Currently, the simple eddy diffusion scheme following Tiedtke (1984) is used in the global forecast system (GFS) of the Central Weather Bureau (CWB).

In this paper, we adopt a shallow cumulus parameterization scheme of Li and Young (1993). Their scheme considers cloud root effects, condensation-evaporation cycle by using conserved variables of liquid water potential temperature and total water content, and includes an empirical nonlocal component to represent cumulus scale large eddies (referred to as KNL). The empirical data (Bougeault 1981) was from a 3-dimensional (3D) moist LES for trade winds.

Experiments are conducted using shallow cumulus schemes that considering: (1) local transfers only with a cumulus eddy exchange coefficient (Kcu) constant with height (CONTROL), (2) local transfers with height-varying Kcu extending downward to surface to include cloud root effects (KL) and (3) the same as (2) but including an empirical nonlocal flux component following Li and Young (1993) (KNL) are conducted, respectively, with a single column version and a full-coupled version of the GFS. A dataset for quasi-steady tradewind conditions during the undisturbed BOMEX period will be used for verification in the single column tests. Perpetual numerical simulations initialized by a July condition with CONTROL and KNL are also presented with the full-coupled GFS.

Section 2 and 3 present an overview of PBL cloud effects, the model for testing as well as the design and methodology of the revised shallow cumulus scheme. The initial conditions and large-scale forcing for the single column model are described in Section4. The simulation results using the shallow cumulus schemes with the single column and full-coupled versions of the GFS are given in Section 5. A summary and conclusion is given in Section 6.

2. MODEL

The CWB GFS uses a TKE-e closure dry turbulent diffusion scheme (Wang 1992) to represent small-scale turbulent mixing. More details of the model are given in Wang (1992) and Liou et al. (1997), and references therein. The composite large-scale variables during BOMEX period are used to initialize a single column version of the GFS of CWB with high vertical resolution (50m).

The shallow cumulus-scale heating and moistening rate may be expressed as

$$\left(\frac{\partial}{\partial t}\bar{\theta}\right)_{cu} = -\frac{\partial}{\partial z}\left(\overline{w'\theta_\ell'}\right), \qquad (1)$$

$$\left(\frac{\partial}{\partial t}\bar{q}\right)_{cu} = -\frac{\partial}{\partial z}\left(\overline{w'q_t'}\right) \qquad (2)$$

where $\overline{w'q_t'}$ and $\overline{w'\theta_\ell'}$ are total water and liquid water potential temperature fluxes, respectively.

3. SHALLOW CUMULUS SCHEME

From the flux budget equations of $\overline{w'q_t'}$ and $\overline{w'\theta_\ell'}$ (details see Li and Young 1993), if the molecular fluxes, Coriolis term and radiation transfer effects are neglected and a quasi-equilibrium state is further assumed. It can be shown that the cumulus fluxes, which have a downgradient diffusion part and a nonlocal one can be expressed as

$$\overline{w'\phi'} = -K_\phi \frac{\partial\bar{\phi}}{\partial z} + K_\phi \alpha \frac{\partial\bar{\phi}}{\partial z} \qquad (3)$$

where ϕ can be either total water content or liquid water potential temperature. Here, the convective available potential energy (CAPE) of shallow cumulus multiplied by active cumulus cloud coverage can be used to define K_ϕ, which is approximately 6.5 estimated from BOMEX (Li and Young 1993).

For the nonlocal terms, the second term on the r.h.s.. of (3), were obtained from Bougeault's one-dimensional higher-order closure model simulation (1981) and the 3-D large-scale eddy simulation (LES) done by Sommeria and LeMone (1978) where

$$\alpha = \frac{1}{a + bF(z)} \qquad (4)$$

with a = 1, b = 1.5 and F(z) is a parabolic function with maximum magnitude of 1 and zero at cloud top and surface layer to include cloud roots effects.

4. EXPERIMENTAL CASE STUDY FOR SINGLE COLUMN TESTS

During the undisturbed periods of MOMEX (June 22-23, 1969), the composite soundings all show a shallow cool dry mixed layer, conditionally unstable cloud layer and strong inversion above. For instance, during BOMEX, net large-scale processes stabilize the environment by cooling/drying the lower part of the cloud layer and warming/drying the upper part of the cloud layer (Figs. 1 and 2). For the entire cloud layer, net large-scale drying/warming is apparent. In this case, to maintain the steady cloud layer, all the subgrid-scale processes (i.e. small and cumulus scales) should give net cooling and moistening in the cloud layer. Such that the shallow cumulus convection acts to destabilize the entire PBL environment assisted by lower boundary flux forcing through surface evaporation and/or warm sea surface temperature (SST). We diagnose the quasi-steady state simulated by the single column version of the GFS and compare it with the above effects, which are implied by the BOMEX data.

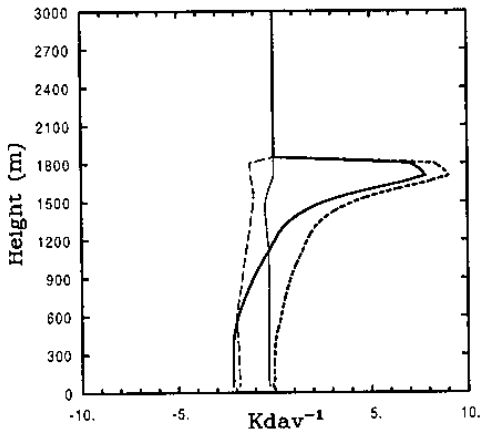

Figure 1. The large-scale heating rates of BOMEX during undisturbed period. Thin line: large-scale advection. Long dashed: net radiation. Heavy long dashed line: large-scale subsidence. Heavy solid line: net large-scale heating rate.

5. RESULTS OF NUMERICAL EXPERIMENTS

5a. Single column tests

(i) Experiment 1: local transfers alone with Kcu constant with height (CONTROL)

We begin our experiment considering local cumulus diffusion only. A maximum value of Kcu 6.5 constant with height is assigned in the whole cloud layer. (Note that a value of 10 of Kcu is used in the currently scheme applied in the GFS.)

Results indicate that the cloud layer can only be maintained in the first two model hours. The time evolution of the simulated cumulus potential temperature fluxes performs unrealistic shape and magnitude in the upper cloud layer (not shown). The flux implies a fairly large cooling in the upper cloud layer resulting in a well-mixed upper cloud layer. The associated heating rates indicate that the cumulus cooling is much larger than large-scale subsidence warming. Thus, a reasonable steady state could not be reached and the cloud layer cannot be maintained as was observed (not shown).

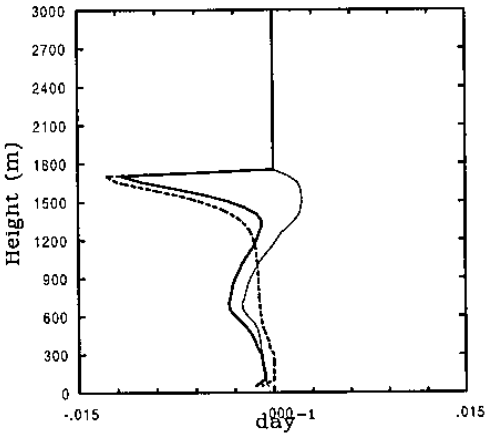

Figure 2. The same as Figure 1 but for moistening rates.

(ii) Experiment 2: local transfers alone but with height varying Kcu (KL)

We repeat simulation as in (i) but with Kcu varying in height with parabolic fit in the cloud layer. A maximum value of 6.5 is assigned in the mid-level between the cloud top and the surface layer (to include cloud roots effects).

The results simulated at 5 hour time evolution of the cumulus potential temperature fluxes perform much more realistic shape and magnitude in the whole cloud layer than that of the experiment (i). The associated small-scale and cumulus warming mainly balances with large-scale cooling in the subcloud layer (Fig. 3). The 5 hours average heating rates indicate that the cumulus cooling rates have larger values (up to -15 K/day) than that of large-scale subsidence warming (9 K/day) at the upper cloud layer while at the lower cloud layer the cumulus heating rates are slightly less than that of the large-scale cooling. The all processes shows the large cooling tendency due to imbalance (–6 K/day) between the large-scale and subgrid scale processes at the upper cloud layer resulting a too cool upper cloud layer when a quasi-steady is reached.

The cumulus water vapor flux has maximum upward transport just above the cloud base indicating cumulus scale drying while the small-scale has strong moistening. The associated cumulus scale moistens the upper cloud layer and dries the lower cloud layer (not shown).

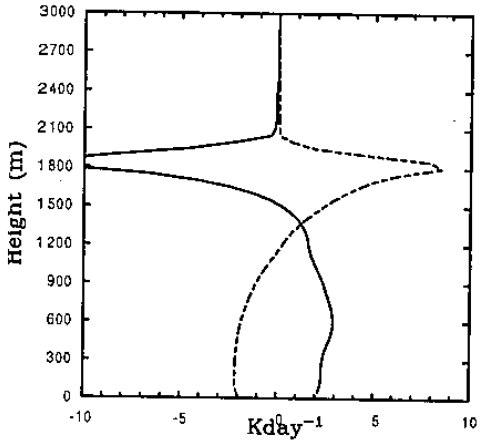

Figure 3. Heating rate (K/day) averaged from the initial time to a steady state with the KL scheme using BOMEX data. Solid: net subgrid scale. Dashed: net large-scale.

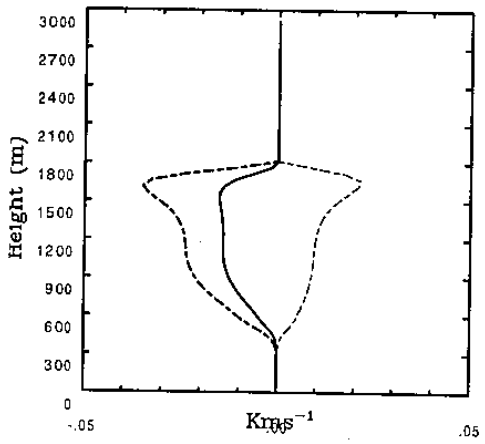

Figure 4. Cumulus scale upgradient (dashed) and downgradient (heavy dashed) parts of liquid water potential temperature fluxes for BOMEX model simulation using KNL scheme in a steady state. The heavy solid line is the net cumulus flux.

(iii) Experiment 3: Nonlocal transfers included

We repeat experiment (ii) focusing on our scheme with nonlocal transfers inclusion (KNL). Figure 4 shows that the upgrading part of cumulus flux cancels almost one half of the local gradient transports. In the upper cloud layer the sharp cooling by the local flux divergence has been smoothed by the nonlocal flux correction. In the subcloud layer and lower cloud layer, the associated small-scale and shallow convection warming nearly balances the net large-scale cooling. The net heating rate of the large-scale and subgrid-scale averaged from the initial time indicates a slight cooling tendency (1-2 K/day) in the upper cloud layer.

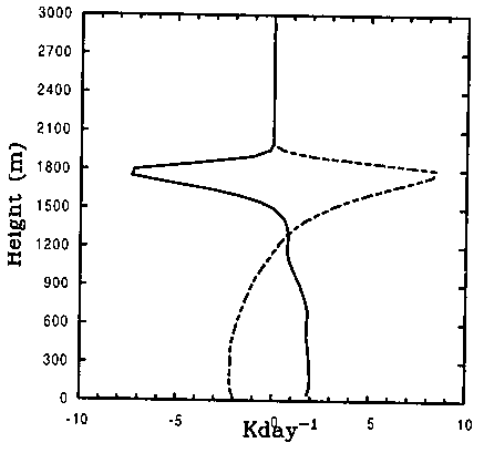

Figure 5. Heating rate averaged from the initial time to steady state with KNL shallow cumulus schemes using BOMEX data.

A good balance between the large-scale and cumulus-scale moisture processes is also found. Continuous small-scale evaporation from the sea surface moistens the subcloud layer while cumulus-scale drying moistens the lower cloud layer through subcloud layer adjustment (not shown). We found that the cloud root effects plays an important role to supply moisture into the cloud layer from the subcloud layer.

5b. Experiment with a full-coupled version of the GFS: preliminary results

Figure 6 shows simulated July monthly-mean precipitation rates using CONTROL and KNL schemes with a full-coupled version of the GFS, respectively. Similar to that in Chen et al. (2000), CONTROL underestimates the values of precipitation rates over eastern equatorial Pacific ITCZ but overestimates the values in the subtropical western Pacific (15-30N) (Fig. 6a). The model with the KNL scheme, on the other hand, simulates much more realistic precipitation rates in both regions compared to that of CONTROL (Fig. 6b). These improvements could be due to the model now simulates more deeper moist PBL over the tradewind regions resulting in more large-scale horizontal moisture transports toward ITCZ. The same month of simulated sea level pressure with KNL shows much realistic subtropical high patterns than that of CONTROL in northern Pacific and the extension of trough is no longer found over southern China and western equatorial Pacific regions (Fig. 7). Detailed analysis is needed to identify these improvements.

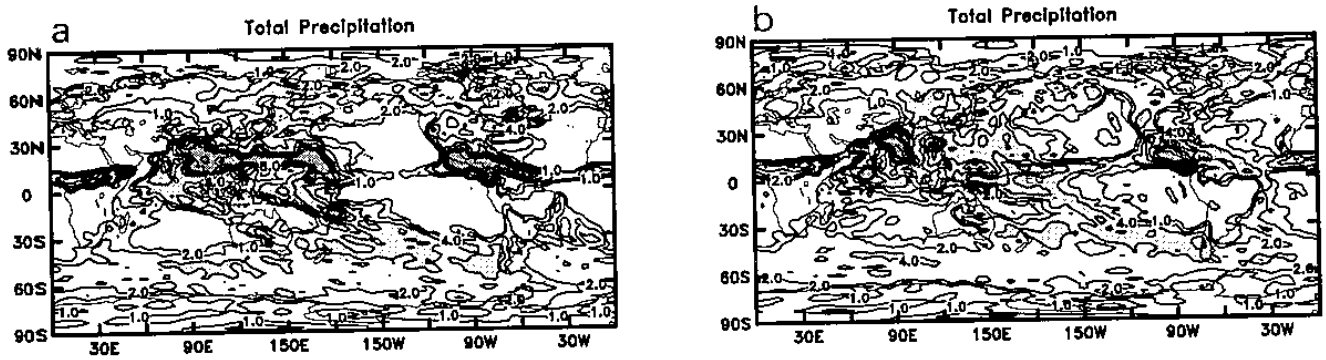

Figure 6. (a) Simulated July mean precipitation rates using CONTROL version. (b) The same as in (a) but with KNL. The contour interval is 1, 2 respectively for the values smaller than 4, and is 4 with values larger than 4 (mm/day).

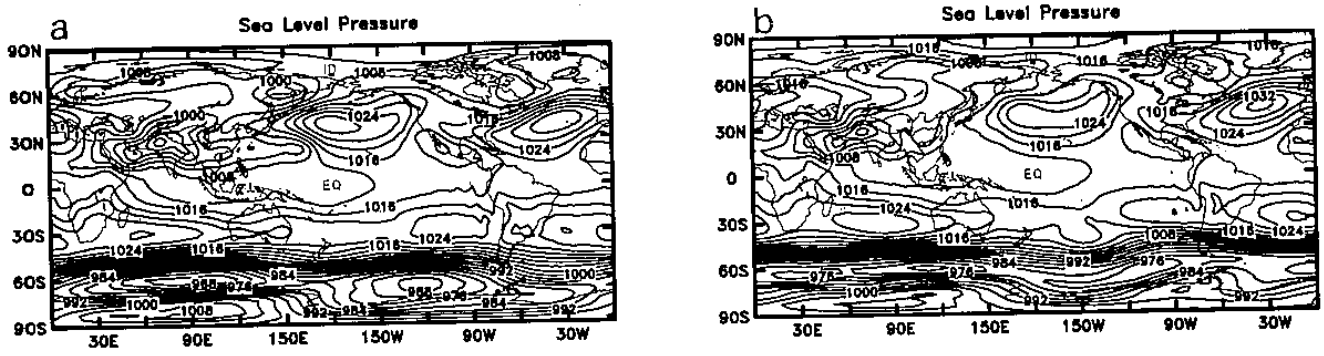

Figure 7. (a) Simulated July mean sea level pressure using CONTROL version. (b) The same as in (a) but with KNL.

6. SUMMARY AND CONCLUSION

A simple cumulus eddy diffusion with a nonlocal flux correction of shallow cumulus parameterization has been presented. The effects of the buoyant cumulus regimes of BOMEX were best described by downgradient liquid water potential temperature and total water mixing, modified by nonlocal transfers, which were the source of positive buoyancy flux. In the upper cloud layer, the upgradient nonlocal cumulus heat fluxes cancel parts of the local gradient transports, so that the sharp cooling rates were smoothed. Thus, a good balance of heating and moistening rates among the large-scale, small-scale and cumulus-scale processes was reached.

We expect the cloud root warming and drying to counteract the small-scale cooling and moistening in the upper subcloud layer. The cloud roots establish a nonlocal transport "pipe" of moisture and heat between the subcloud layer and cloud layer, which can alleviate unrealistic subcloud moistening. We anticipate that nonlocal processes and cloud root effects must be included in the cloud-scale parameterization schemes for stronger buoyant cumulus boundary layers.

Preliminary results simulated with the shallow cumulus scheme plus nonlocal transfers using a full-coupled version of the GFS are very encouraging. The model simulated reasonably good geographical distributions of precipitation rates, sea level pressure and surface latent heat flux in July. Further detailed analysis of the impacts from the revised formulation of the shallow cumulus scheme on the global hydrological processes in the GFS is required.

We found that KNL is simple and useful to be formulated in a GCM. However, since the scheme was

restricted to the trade wind PBL, it could not be generally applied to more active cumulus situations such as over regions of CAO. A theoretical model based on fundamental processes and observed cumulus behavior seemed necessary, and should be considered in future.

Acknowledgments.

The authors wish to thank Drs. Mean-Dean Chen, Chin-Tzu Fong and Jyh-Wen Hwu for their helps. This research was funded under CWB89-3M-03. Model integrations were performed at the computer facilities at Central Weather Bureau, Taipei, Taiwan, R.O.C.

REFERENCE

Betts, A. K. and Miller 1986: A new convective adjustment scheme I: Observational and theoretical basis. Quart. J. Roy. Meteor. Soc., 112, 677-691.

Bougeault, Ph., 1981a: Modeling the trade-wind cumulus boundary layer. Part I: Testing the ensemble cloud relations against numerical data. J. Atmos. Sci., 38, 2414-2428.

Bougeault, Ph., 1981b: Modeling the trade-wind cumulus boundary layer. Part II: A high-order one-dimensional model., J. Atmos. Sci., 38, 2429-2439.

Chen, J-M et. al., 200: Climate Characteristics of the CWB Global Forecast System: Hydrological Processes and Atmospheric Circulation. Accepted to TAO, 2000.

LeMone, M. A., and W. T. Pennel, 1976: The relationship of trade wind cumulus distribution to subcloud layer fluxes and structure. Mon. Wea. Rev.,104, 524-539.

Li, J.-L. F. and J. A. Young, 1993: Modeling the interactions of shallow cumulus clouds with large-scale boundary layer fields. 6th conference on climate variations, 23-28 January 1994, 24-243.

Liou, C-S, et al., 1997: The second-generation global forecast system at the Central Weather Bureau in Taiwan. Wea. Forecasting, 12, 653-663.

Riehl, H, T. C. Yeh, J. S. Maikus and N. E. La Seur, 1951: The North-East trade of the Pacific Ocean. Quart. J. Roy. Meteor. Soc., 77, 598-626.

Sommeria, G. and A. M. LeMone, 1978: Direct testing of three-dimensional model of the planetary boundary layer against experimental data. J. Atmos. Sci.,35, 25-39.

Song, S.-T., and Y. Ogura, 1980: Response of tradewind cumuli to large-scale processes. J. Atmos. Sci., 37, 2035-2050.

Tiedtke, M., 1984: The sensitivity of the time-mean large-scale flow to cumulus convection in the ECMWF model. ECMWF Workshop on Convection in large-scale Numerical Models, 28 Nov.1 Dec., 1983, 297-316.

Wang, F-J, 1992: A numerical study on multilevel boundary layer parameterization with E-e turbulence closure. Atmos. Sci., 20, 217-232.